Supporting Information

Nishimura et al. 10.1073/pnas.1003553107

SI Text

SI Materials and Methods. ***Plasmid construction.*** The cDNAs of human $G\alpha_q$ were amplified and subcloned into pCMV5. Mutants of $G\alpha_q$ (R60K, L78N, V184S, I190N, and P193C) were generated by site-directed PCR mutagenesis. A soluble and functional chimeric protein, $G\alpha_{i/q}$, which comprises the N-terminal helix (residues 1–28) of rat $G\alpha_{i1}$, the Arg-Ser linker, and the core domain of mouse $G\alpha_q$ (residues 37–359) was generated by overlapping PCR as previously described (1).

X-ray data collection. For X-ray data collection, the crystal was mounted on a rayon loop and flash-frozen in liquid nitrogen. The X-ray data were collected at SPring-8 on beamline BL41XU. The crystal was maintained at 100 K in a nitrogen stream during exposure to the X-ray beam with a wavelength of 1.00 Å. Diffraction from a total oscillation range of 180° was recorded by the charge-coupled device detector (ADSC Quantum 315). The dataset was indexed and merged using the HKL2000 program suite (2).

Structure determination. The phases were determined by the molecular replacement (MR) method using the GDP + AlF_4^- form of the $G\alpha_{i/q}$ subunit (PDB ID: 2BCJ) (1) and the Gβγ subunits (PDB ID: 1GP2) (3) as a search model. Two independent MR calculations using the $G\alpha_{i/q}$ and Gβγ coordinates were performed by the PHASER (4) program, which successfully gave solutions corresponding to the known architecture of the heterotrimer. One complex was included in the asymmetric unit of the crystal. In the model building, the structure of the heterotrimer was at first refined by CNS (5). The inhibitor model was then built into the residual electron-density map using the graphic program Coot (6). In this process, the ring-shaped densities with an extended body (corresponding to the cyclic backbone with the YM-254890 subregion) were traced by two different orientations of an inhibitor structure, a clockwise one and an anticlockwise one, as well as with several different conformations of the subregion. Only the present structure fully fitted into the densities accompanied with the lowest R-values. The structure was finally refined by REFMAC with TLS parameterization (7). The figures were prepared using PyMOL (DeLano Scientific).

Trypsin protection assay. 293T cells were transfected with each Gα. At 48 h posttransfection, the cells were washed with PBS and lysed with a lysis buffer (20 mM Hepes-NaOH pH 8.0, 100 mM NaCl, 3 mM $MgCl_2$, 1 mM EDTA, 1 mM DTT, 10 μM GDP, and 0.5% Lubrol-PX). Lysates were cleared by centrifugation at 14,000 g for 10 min, and supernatants were pretreated with or without 10 μM YM-254890 for 15 min at 30 °C. Next, supernatants (1.5 mg/mL) were incubated with or without AlF_4^- (10 mM $MgCl_2$, 5 mM NaF, and 50 μM $AlCl_3$) for 15 min at 30 °C and then treated with 5 μg/mL TPCK-trypsin for 20 min at 30 °C. The reactions were stopped by the addition of Laemmli sample buffer. The digestion of $G\alpha_q$ or $G\alpha_{14}$ was detected using an anti-$G\alpha_{q/11}$ antibody (Santa Cruz Biotechnology) or anti-$G\alpha_{14}$ antibody (Gramsch Laboratories) that recognizes the C-terminal tail of the corresponding protein.

AlF_4^--induced Gα dissociation from Gβγ. The assay was performed as previously described by Yamaguchi et al. (8) with some modification. Briefly, 293T cells were transfected with each Gα, $G\beta_1$, and FLAG-$G\gamma_2$. At 48 h posttransfection, the cells were pretreated with or without 10 μM YM-254890 for 30 min and incubated with or without AlF_4^- for an additional 2 h. The cells were then washed with PBS and lysed with lysis buffer with or without 10 μM YM-254890 and AlF_4^-. Lysates were cleared by centrifugation at 14,000 g for 10 min, and the supernatants were then incubated with the anti-FLAG antibody and protein G-Sepharose for 1 h. Immunoprecipitates were washed three times with lysis buffer and treated with Laemmli sample buffer.

1. Tesmer VM, Kawano T, Shankaranarayanan A, Kozasa T, Tesmer JJ (2005) Snapshot of activated G proteins at the membrane: The Galphaq–GRK2–Gbetagamma complex. *Science* 310:1686–1690.
2. Otwinowski Z, Minor W (1997) Processing of X-ray diffraction data collected in oscillation mode. *Methods Enzymol* 276:307.
3. Wall MA, et al. (1995) The structure of the G protein heterotrimer Gi alpha 1 beta 1 gamma 2. *Cell* 83:1047–1058.
4. McCoy AJ, Grosse-Kunstleve RW, Storoni LC, Read RJ (2005) Likelihood-enhanced fast translation functions. *Acta Crystallogr D* 61:458–464.
5. Brunger AT, et al. (1998) Crystallography & NMR system: A new software suite for macromolecular structure determination. *Acta Crystallogr D* 54:905–921.
6. Emsley P, Cowtan K (2004) Coot: Model-building tools for molecular graphics. *Acta Crystallogr D* 60:2126–2132.
7. Winn MD, Murshudov GN, Papiz MZ (2003) Macromolecular TLS refinement in REFMAC at moderate resolutions. *Methods Enzymol* 374:300–321.
8. Yamaguchi Y, Katoh H, Negishi M (2003) N-terminal short sequences of alpha subunits of the G12 family determine selective coupling to receptors. *J Biol Chem* 278:14936–14939.

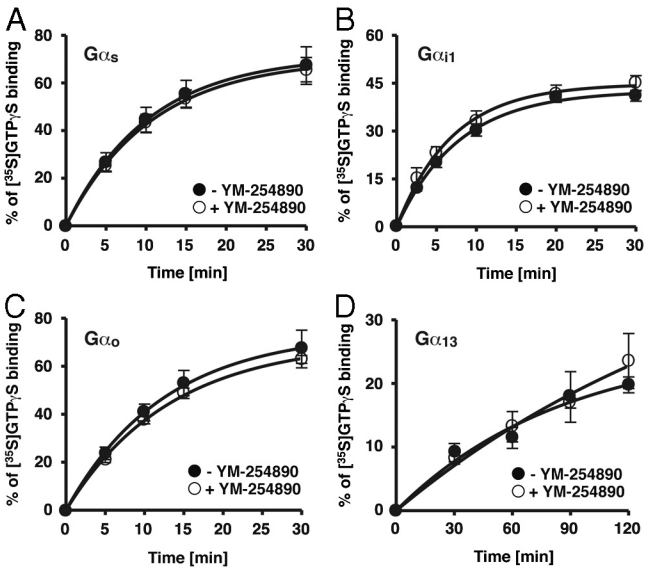

Fig. S1. The α subunit selectivity of YM-254890. Purified $G\alpha_s$ (*A*), $G\alpha_{i1}$ (*B*), $G\alpha_o$ (*C*), or $G\alpha_{13}$ (*D*) at a concentration of 100 nM was preincubated with (open circles) or without (filled circles) 10 μM YM-254890 for 3 min, and GTPγS binding assay was performed. Each value represents the mean ± S.D. from three independent experiments.

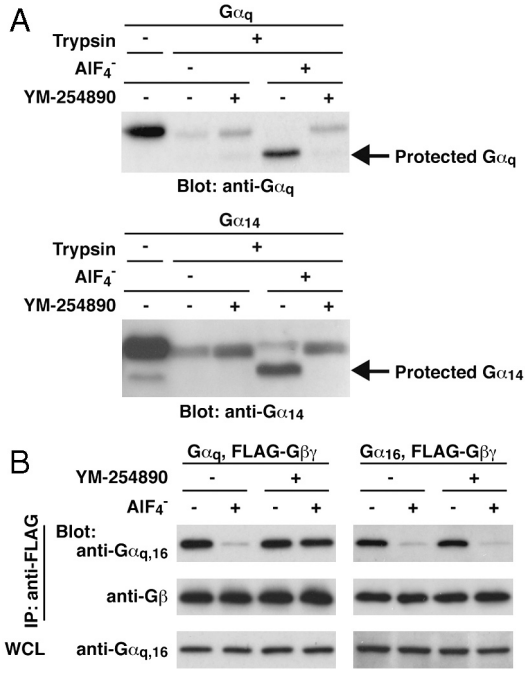

Fig. S2. YM-254890 sensitivity of $G\alpha_{14}$ and $G\alpha_{16}$. The AlF_4^--induced conformational changes in $G\alpha_{14}$ and $G\alpha_{16}$ were evaluated with the trypsin protection assay (*A*) or the dissociation from Gβγ (*B*), respectively. (*A*) 293T cells were transfected with $G\alpha_q$ or $G\alpha_{14}$ plasmid. Cell lysate was pretreated with or without 10 μM YM-254890 and then incubated with or without AlF_4^-. Gα in the lysate was digested with trypsin. The trypsin sensitivities of $G\alpha_q$ and $G\alpha_{14}$ were analyzed by immunoblotting using anti-$G\alpha_q$ and anti-$G\alpha_{14}$ antibodies, respectively. Partially protected 38 kDa products of $G\alpha_q$ and $G\alpha_{14}$ are shown as Protected $G\alpha_q$ and Protected $G\alpha_{14}$, respectively. (*B*) 293T cells transfected with Gα, $G\beta_1$, and FLAG-$G\gamma_2$ were preincubated with or without 10 μM YM-254890. After 30 min, 293T cells were treated with or without AlF_4^- for an additional 2 h. The whole-cell lysate (WCL) was prepared and incubated with an anti-FLAG antibody and protein G-Sepharose. Coimmunoprecipitation of $G\alpha_q$ or $G\alpha_{16}$ with FLAG-$G\beta_1\gamma_2$ was detected with anti-$G\alpha_q$ and anti-$G\alpha_{16}$ antibodies, respectively.

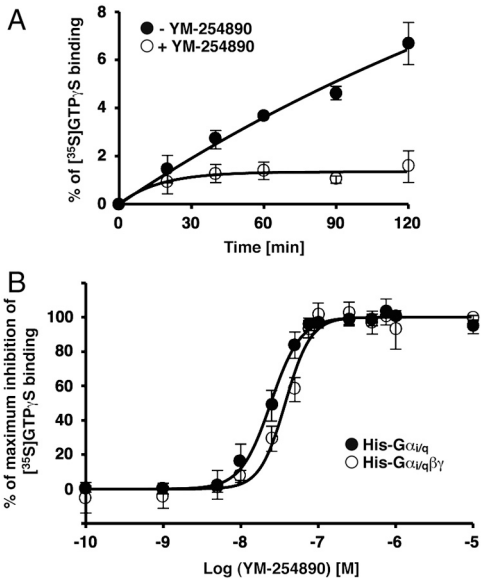

Fig. S3. Comparison of YM-254890 sensitivity between $G\alpha_{i/q}$ monomer and $G\alpha_{i/q}\beta\gamma$ heterotrimer. (*A*) Inhibition of GTPγS binding to His-$G\alpha_{i/q}\beta\gamma$ heterotrimer. Purified His-$G\alpha_{i/q}\beta\gamma$ (100 nM) was preincubated with (open circles) or without (filled circles) 10 μM YM-254890 for 3 min, and the GTPγS binding assay was performed. (*B*) Comparison of dose-dependent inhibition of GTPγS binding to His-$G\alpha_{i/q}$ and His-$G\alpha_{i/q}\beta\gamma$. Purified His-$G\alpha_{i/q}$ (filled circles) or His-$G\alpha_{i/q}\beta\gamma$ (open circles) was preincubated with the indicated concentration of YM-254890, and the GTPγS binding assay was performed for 120 min. Each value represents the mean ± S.D. from three independent experiments.

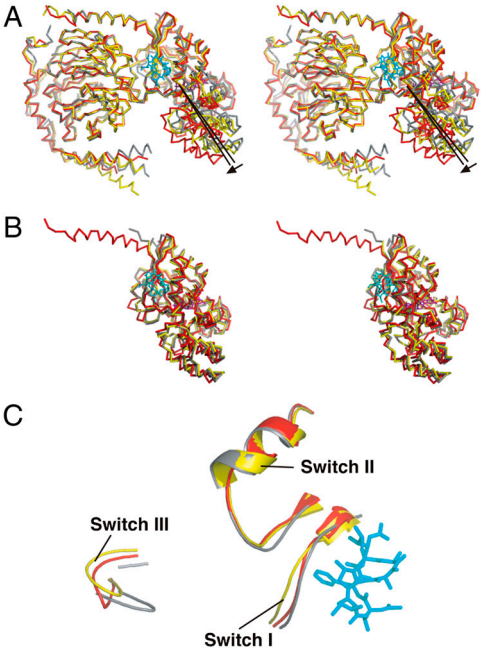

Fig. S4. Comparison of overall structure of $G\alpha_{i/q}\beta\gamma$-YM-254890 with those of other $G\alpha\beta\gamma$. (*A*) Stereo view of the $G\alpha_{i/q}\beta_1\gamma_2$ (red), which is bound to GDP (purple) and YM-254890 (cyan), superimposed on $G\alpha_{i1}\beta_1\gamma_2$ (yellow) (1) and $G\alpha_{t/i}\beta_1\gamma_1$ (gray) (2). The helical domain of $G\alpha_{i/q}$ may be rotated through the hinge regions (Linker 1 and Switch I) compared with those of $G\alpha_{i1}$ and $G\alpha_{t/i}$. (*B*) Stereo view of the $G\alpha_{i/q}$ (red), which is bound to GDP and YM-254890, superimposed on the $G\alpha_{i/q}$ bound to GDP and AlF_4^- from $G\alpha_{i/q}$-GRK2-Gβγ complex (yellow) (3) and $G\alpha_{i/q}$-p63RhoGEF-RhoA complex (gray) (4). (*C*) Close-up view of the three switch regions of $G\alpha_{i/q}$. The conformations of three switch regions of $G\alpha_{i/q}\beta\gamma$ bound to YM-254890 are essentially the same as those of $G\alpha_{i1}\beta\gamma$ and $G\alpha_{t/i}\beta\gamma$, which display the typical inactive GDP-bound conformation.

1 Wall MA, et al. (1995) The structure of the G protein heterotrimer Gi alpha 1 beta 1 gamma 2. *Cell* 83:1047–1058.
2 Lambright DG, et al. (1996) The 2.0 Å crystal structure of a heterotrimeric G protein. *Nature* 379:311–319.
3 Tesmer VM, Kawano T, Shankaranarayanan A, Kozasa T, Tesmer JJ (2005) Snapshot of activated G proteins at the membrane: The Galphaq–GRK2–Gbetagamma complex. *Science* 310:1686–1690.
4 Lutz S, et al. (2007) Structure of Galphaq–p63RhoGEF–RhoA complex reveals a pathway for the activation of RhoA by GPCRs. *Science* 318:1923–1927.

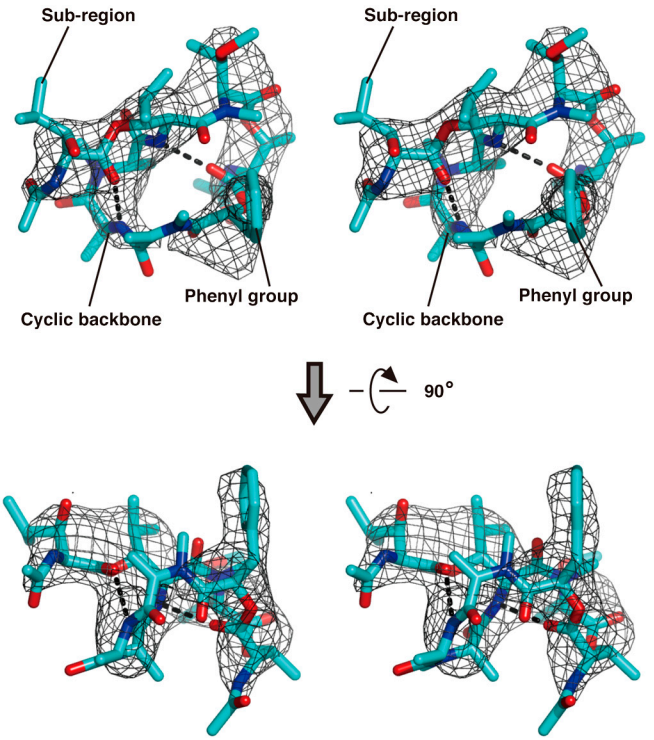

Fig. S5. Stereo view of the structure model of YM-254890 bound to the heterotrimer. The $|F_o|$-$|F_c|$ omit electron-density map contoured at 3.3σ (gray mesh) is superimposed. The map was calculated without the contribution of YM-254890. Oxygen and nitrogen are shown in red and blue, respectively. The hydrogen bonds within a distance of 3.3 Å are shown as dashed lines.

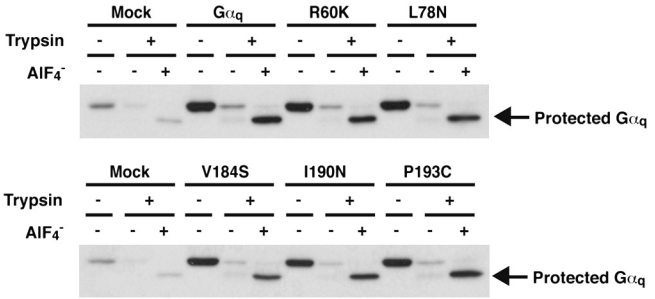

Fig. S6. Trypsin protection assay of each $G\alpha_q$ mutant. 293T cells were transfected with each $G\alpha_q$ mutant plasmid. Cell lysate was preincubated with or without AlF_4^-, and then $G\alpha_q$ was digested with trypsin.

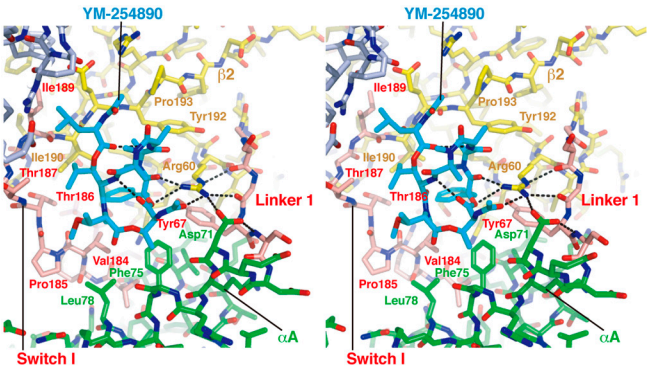

Fig. S7. Stereo view of the interaction between YM-254890 and $G\alpha_{i/q}\beta\gamma$. $G\alpha_{i/q}\beta\gamma$-YM-254890 complex depicted as a stick model is shown in the same orientation as Fig. 3*E*. GTPase domain, helical domain, and two linkers of $G\alpha_{i/q}$ are shown in yellow, green, and light red, respectively. Gβ and YM-254890 are light blue and cyan, respectively. Oxygen and nitrogen are shown in red and blue, respectively. Hydrogen bonds are shown as dashed lines.

Table S1. Crystallographic data for the $G\alpha_{i/q}\beta\gamma$-YM-254890 complex

X-ray data	
Space group	$I4_1$
Cell parameters [Å]	$a = b = 173.3$, $c = 60.9$
Resolution [Å] *	20–2.9 (3.0–2.9)
Mosaicity	0.2–0.3
V_M[Å^3/Da]/$V_{solvent}$ [%]	2.59/47.5
Reflections, total/unique	80,301/19,018
Completeness [%]	94.1 (76.9)
$\langle I/\sigma_I \rangle$	11.1 (2.4)
Redundancy	4.2 (4.1)
R_{merge} [%]	5.9 (52.6)
Refinement	
Number of residues included	
$G\alpha_q$	342 (of 355)
$G\beta$	330 (of 340)
$G\gamma$	50 (of 78)
Number of atoms	5,829
R_{work}/R_{free} [%] †	25.9/31.5
Ramachandran plot [%]	
Most favored	81.6
Additionally allowed	16.4
Generously allowed	1.8
Disallowed	0.2 (Thr87 of $G\beta$)
Average B-factor [Å^2]	
$G\alpha_q$	91.1
$G\beta$	91.2
$G\gamma$	93.1
GDP	90.7
YM-254890	101.7
R.m.s. bond length [Å], angles [°]	0.011, 1.2

*Numbers in parentheses refer to statistics for the outer resolution shell.

†$R_{work} = \Sigma||F_{obs}| - |F_{calc}||/\Sigma|F_{obs}|$. R_{free} is the same as R_{work} except for a 5% subset of all reflections that were never used in the crystallographic refinement.